Matrix Biology 122 (2023) 10–17

Contents lists available at ScienceDirect

Matrix Biology

journal homepage: www.elsevier.com/locate/matbio

Global, but not chondrocyte-specific, MT1-MMP deficiency in adult mice causes inflammatory arthritis

Xiao-dan Xia [a,b,1], Govind Gill [b,1], Haiming Lin [c,d,1], Daniela M. Roth [c], Hong-mei Gu [b], Xiang-jiang Wang [a], Feng-yi Su [a], Adekunle Alabi [b], Maria Alexiou [c], Ziyang Zhang [b], Gui-qing Wang [a,*], Daniel Graf [c,*], Da-wei Zhang [b,*]

[a] Department of Orthopedics, the Sixth Affiliated Hospital of Guangzhou Medical University, Qingyuan People's Hospital, Qingyuan, Guangdong, China
[b] Department of Pediatrics, Group on the Molecular and Cell Biology of Lipids, Faculty of Medicine and Dentistry, University of Alberta, Edmonton, Alberta, Canada
[c] Department of Dentistry & Dental Hygiene, Faculty of Medicine and Dentistry, University of Alberta, Edmonton, Alberta, Canada
[d] Department of Orthopaedics, The First Affiliated Hospital of Shantou University Medical College, Shantou, Guangdong, China

ARTICLE INFO

Keywords:
LRP1
Collagen
Extracellular matrix
Metalloproteinase
Musculoskeletal syndrome

ABSTRACT

Membrane-type I metalloproteinase (MT1-MMP/MMP14) plays a key role in various pathophysiological processes, indicating an unaddressed need for a targeted therapeutic approach. However, mice genetically deficient in *Mmp14* show severe defects in development and growth. To investigate the possibility of MT1-MMP inhibition as a safe treatment in adults, we generated global *Mmp14* tamoxifen-induced conditional knockout (*Mmp14*^{kd}) mice and found that MT1-MMP deficiency in adult mice resulted in severe inflammatory arthritis. *Mmp14*^{kd} mice started to show noticeably swollen joints two weeks after tamoxifen administration, which progressed rapidly. *Mmp14*^{kd} mice reached a humane endpoint 6 to 8 weeks after tamoxifen administration due to severe arthritis. Plasma TNF-α levels were also significantly increased in *Mmp14*^{kd} mice. Detailed analysis revealed chondrocyte hypertrophy, synovial fibrosis, and subchondral bone remodeling in the joints of *Mmp14*^{kd} mice. However, global conditional knockout of MT1-MMP in adult mice did not affect body weight, blood glucose, or plasma cholesterol and triglyceride levels. Furthermore, we observed substantial expression of MT1-MMP in the articular cartilage of patients with osteoarthritis. We then developed chondrocyte-specific *Mmp14* tamoxifen-induced conditional knockout (*Mmp14*^{chkd}) mice. Chondrocyte MT1-MMP deficiency in adult mice also caused apparent chondrocyte hypertrophy. However, *Mmp14*^{chkd} mice did not exhibit synovial hyperplasia or noticeable arthritis, suggesting that chondrocyte MT1-MMP is not solely responsible for the onset of severe arthritis observed in *Mmp14*^{kd} mice. Our findings also suggest that highly cell-type specific inhibition of MT1-MMP is required for its potential therapeutic use.

Introduction

Membrane-type I metalloproteinase (MT1-MMP/MMP14), encoded by the *MMP14* gene, is a Zn^{2+}-dependent endopeptidase that belongs to a six-member family of membrane-type MMPs. It is synthesized as a zymogen and activated through cleavage by furin-like convertase. MT1-MMP is ubiquitously expressed and cleaves extracellular matrix (ECM) and non-matrix substrates. The metalloproteinase is expressed in various types of cancer cells and promotes cancer metastasis [1,2]. Furthermore, MT1-MMP promotes LDLR cleavage and increases plasma LDL-C levels, exacerbating the progression of atherosclerosis [3]. It also cleaves the insulin receptor and reduces insulin sensitivity in aged mice [4]. Neuronal MT1-MMP proteolytically cleaves GDNF family receptor-α-like and stimulates food intake and weight gain in mice fed a high-fat diet [5]. Additionally, MT1-MMP is highly expressed in cartilage and synoviocytes during arthritis and mediates synovial fibroblast invasion [6,7]. Therefore, MT1-MMP inhibition presents as a promising therapeutic target.

Notably, constitutive global *Mmp14* knockout mice display multiple severe abnormalities during development and die 3–4 weeks after birth [8,9]. Broad-spectrum MMP inhibitors also cause severe side effects in patients, such as musculoskeletal syndrome (MSS), mainly due to poor

* Corresponding authors.
E-mail addresses: wangguiqing@gzhmu.edu.cn (G.-q. Wang), dgraf@ualberta.ca (D. Graf), dzhang@ualberta.ca (D.-w. Zhang).
[1] These authors contributed equally to this work.

https://doi.org/10.1016/j.matbio.2023.08.003
Received 23 April 2023; Received in revised form 17 August 2023; Accepted 17 August 2023
Available online 19 August 2023

substrate selectivity. However, further studies suggest that MMP-1 and ADAM17, but not MT1-MMP, contribute to MSS [10–12]. Additionally, mice with monocytes/macrophages, hepatocytes, or epidermis-specific MT1-MMP knockout are indistinguishable from wild-type littermates without challenge [3,13,14]. Given that treatment of many patients with diseases, such as cardiovascular disease and arthritis, occur primarily in adulthood, we developed global MT1-MMP tamoxifen-induced conditional knockout mice (*Mmp14*^{kd}) to assess the impact of systemic MT1-MMP inhibition in adult mice. We found that global conditional knockout of MT1-MMP in adult mice resulted in severe arthritis but had no significant effect on body weight, blood glucose, or plasma lipid levels. In addition, we observed substantial expression of MT1-MMP in the cartilage of patients with osteoarthritis (OA). To further understand the role of MT1-MMP in the development of arthritis in adult mice, we generated chondrocyte-specific MT1-MMP tamoxifen-induced conditional knockout mice (*Mmp14*^{chkd}) and found that chondrocyte MT1-MMP deficiency in adult mice did not lead to inflammatory arthritis. These findings suggest that chondrocyte MT1-MMP is likely not the sole driver for the development of severe arthritis in adult *Mmp14*^{kd} mice.

Results and discussion

Global Mmp14 conditional knockout mice

To generate inducible *Mmp14*^{kd} mice, *Mmp14*^{flox} mice were bred with mice carrying the tamoxifen-inducible Cre recombinase (Cre-ER^{T2}) under the control of the endogenous mouse Gt(ROSA)26Sor promoter (ROSA26CreER^{T2}) (**Figure S1A**). Heterozygous ROSA26Cre-*Mmp14*^{flox} mice contained Cre-ER^{T2}, and both loxP and wild-type *Mmp14* bands, whereas homozygous mice contained Cre-ER^{T2} and only loxP *Mmp14* bands (**Figure S1B**). Exon 2 and exon 4 of the mouse *Mmp14* gene containing the prodomain and catalytic domain were flanked by loxP sites. The floxed fragment was lost in tamoxifen-administered *Mmp14*^{kd} mice but not in olive oil-injected control ROSA26-Cre/ER^{T2}-*Mmp14*^{flox} mice (**Figures S1C**). PCR data showed a 694 bp product, which was obtained from Cre-mediated recombination of the *Mmp14* gene, only in tissues of tamoxifen-administered mice (**Figure S1D**). qRT-PCR data confirmed that *Mmp14* expression was significantly reduced in *Mmp14*^{kd} mouse tissues, including the heart, kidney, liver, lung, spleen, and intestine (Fig. 1**A**), indicating efficient conditional knockout of *Mmp14*.

Two weeks after tamoxifen injection, adult *Mmp14*^{kd} mice started to show red and swollen joints and paws compared with control mice (Fig. 1**B**). *Mmp14* deficiency significantly increased the thickness of hind paws (Figs. 1**C and D**), and the size of the third digit of forepaws (**Figures S2A and B**). Joints of *Mmp14*^{kd} mice also lost their flexibility and became stiff (Figs. 1**E and F**). Furthermore, unlike the yellowish synovium of control mice, the synovium of *Mmp14*^{kd} mice was red 6 weeks post-tamoxifen administration (Figs. 1**G and H**), suggesting synovitis. Consistently, plasma TNF-α levels were significantly elevated in *Mmp14*^{kd} mice (Fig. 1**I**). Additionally, micro-computed tomography (μCT) showed bone destruction and subchondral remodeling in *Mmp14*^{kd} mice 6 weeks post tamoxifen administration compared to mice injected with olive oil, suggesting advanced arthritis with stages of bone remodeling (Figs. 1**J and K**). Arthritis symptoms advanced rapidly in *Mmp14*^{kd} mice when assessed using clinical arthritis scoring [15], which were not improved by buprenorphine. Almost all *Mmp14*^{kd} mice reached a humane endpoint and were euthanized by 6 to 8 weeks post-tamoxifen administration (**Figure S2C**). Thus, MT1-MMP deficiency in adult mice leads to a form of severe inflammatory arthritis, consistent with findings in global constitutive *Mmp14* knockout mice [8,9].

We then conducted a detailed analysis of mouse knee joints. Masson's trichrome staining of the joint capsule demonstrated normal synovial lining in control mice post-oil administration (Fig. 2**A**). On the other hand, *Mmp14*^{kd} mice displayed thickening of the synovial membrane as early as 2 weeks post tamoxifen administration (Fig. 2**B, red arrows**), which became more severe at 4 weeks (Fig. 2**C**). At the 8-week time point, the fat pad under the normal synovial lining essentially disappeared, and the soft tissues were replaced with fibrotic tissue in *Mmp14*^{kd} mice (Fig. 2**D**). Additionally, *Mmp14*^{kd} mice appeared to have

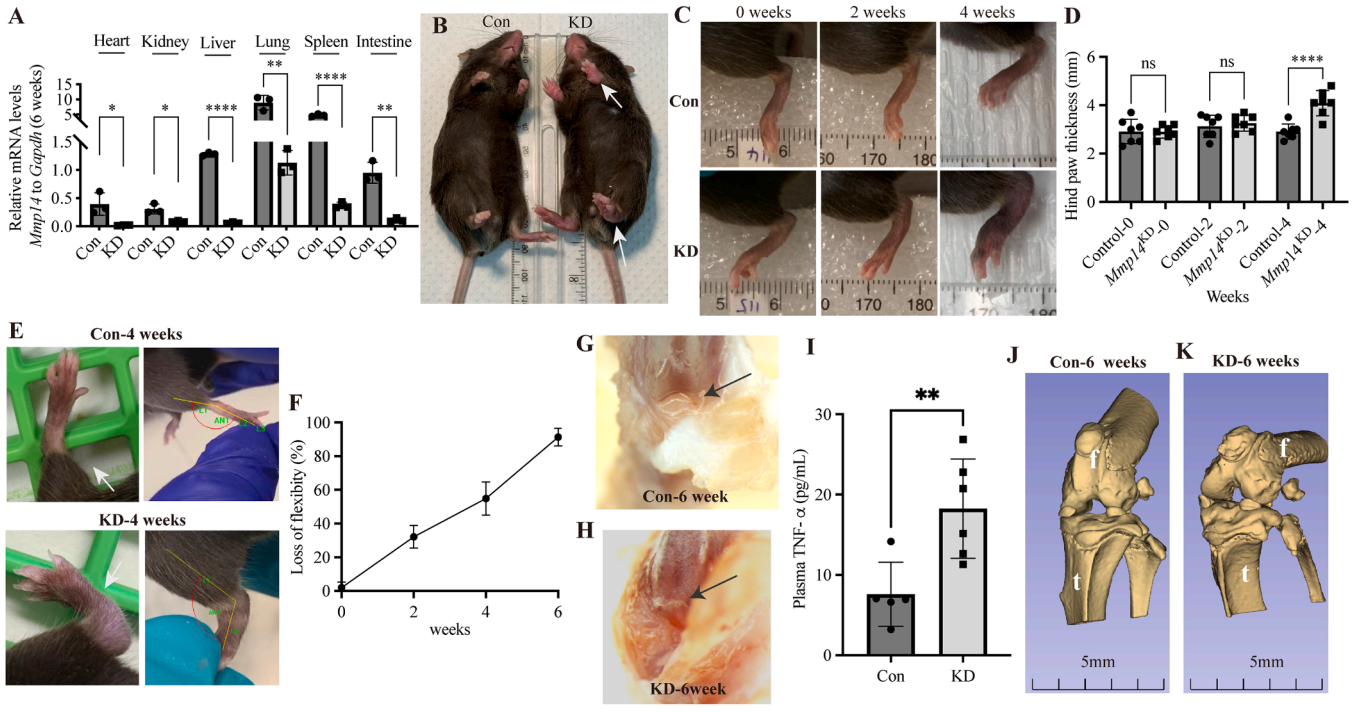

Fig. 1. Arthritis in *Mmp14*^{kd} mice. Mice (10–12 weeks old) were injected with olive oil (Con) or tamoxifen (KD) and then analyzed at the indicated time of post-injection. **A.** qRT-PCR of different tissues ($n = 3$). **B.** Picture of mice 4 weeks post-injection. **C and D.** The thickness of the hind paw ($n = 7$). **E and F.** Joint flexibility ($n = 7$). **G and H.** Images of mouse joints showing synovial membrane (arrow). **I.** Plasma TNF-α levels (con, $n = 5$; KD, $n = 6$). **J and K.** Reconstruction of μCT images ($n = 3$). Representative images were shown. Similar results were observed in other samples in the same group. ns=no significant. f, femur; m, meniscus; t, tibia.

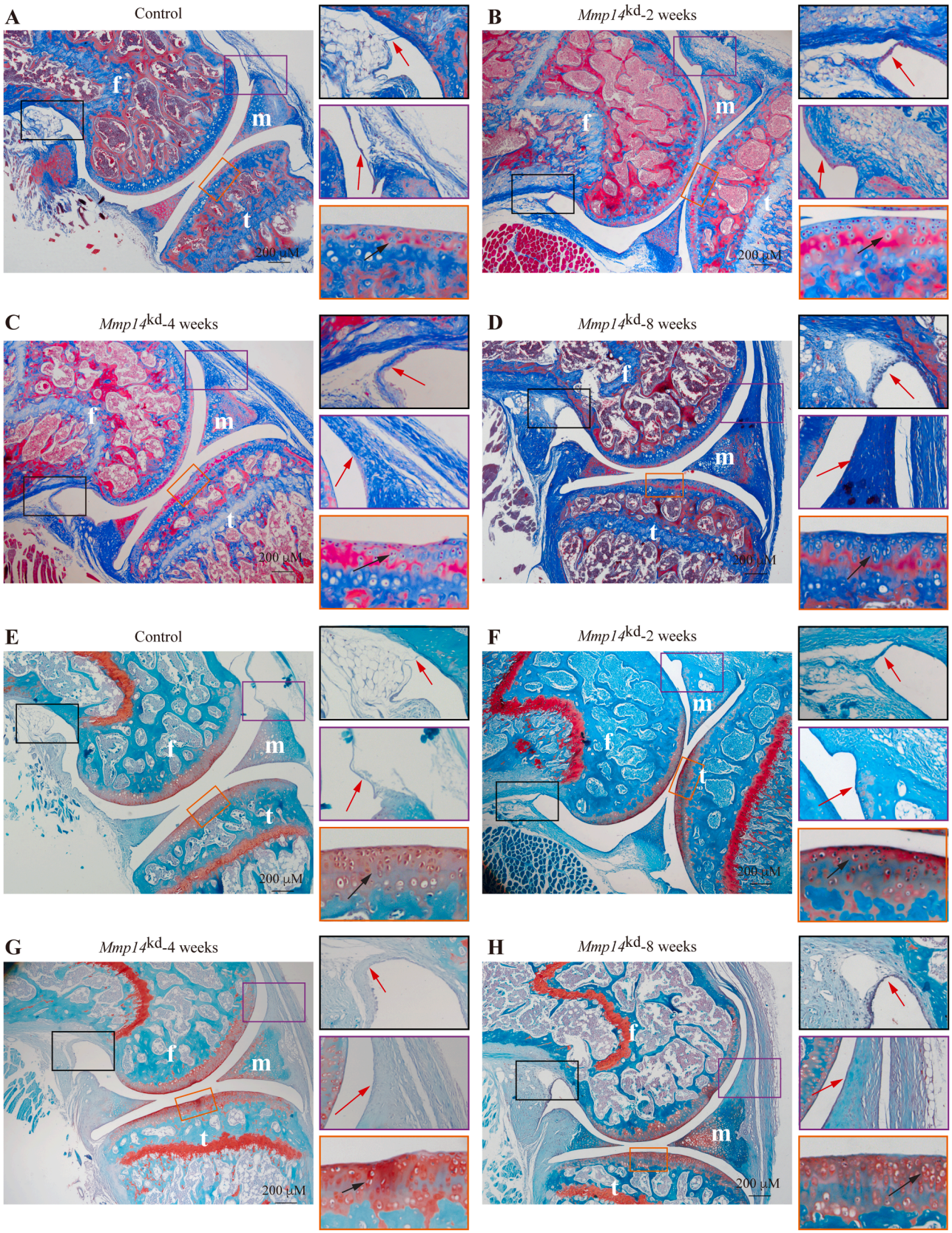

Fig. 2. Histology of *Mmp14*^{kd} mice. Mice (10–12 weeks old) were injected with olive oil (Control) or tamoxifen (*Mmp14*^{kd}) and then analyzed at the indicated time of post-injection ($n = 5$). **A to D**. Masson's trichrome staining. Sections were stained with staining solutions from Servicebio (Wuhan, China). **E to H.** Safranin O/Fast Green staining. Sections were stained with solutions from Solarbio (Beijing, China). Enlarged views showed synovial membrane (red arrows) and chondrocytes (black arrows). Representative images were shown. Similar results were observed in other samples in the same group. f, femur; m, meniscus; t, tibia.

hypertrophic chondrocytes at the 4 and 8-week time points (Figs. 2**C and D, black arrows**). These observations were confirmed using Safranin-O/fast-green staining of adjacent sections (Figs. 2**E-H**). Holmbeck et al. observed fibrosis of connective tissues in global constitutive *Mmp14* knockout mice. The authors suggested that MT1-MMP knockout impaired remodeling during growth, which might lead to arthritis in constitutive *Mmp14* knockout mice [9]. Here, we observed synovial hyperplasia, progressive fibrosis, and hypertrophic chondrocytes in conditional *Mmp14* knockout mice during adulthood, suggesting that MT1-MMP plays a critical role in maintaining synovial and chondrocyte homeostasis, although the precise underlying mechanisms remain unclear.

Synoviocytes include macrophage-like and fibroblast-like cells. Synovial macrophages are primarily derived from monocytes [16]. Mice deficient in monocyte/macrophage *Mmp14* do not display arthritis [13], suggesting that *Mmp14* deficiency in synovial macrophages does not, or is insufficient to cause such overt arthritis. Synovial fibroblasts constitute the majority of cells in the intima, and their overproliferation and invasion cause progressive joint destruction in inflammatory arthritis [17]. MT1-MMP is highly expressed in the rheumatoid synovial lining cells and promotes their invasion into the joint capsule [6,7]. *Mmp14* deficiency in adult mice led to joint stiffness, which is consistent with the phenotype observed in patients treated with MMP inhibitors. Experiments are ongoing to investigate how MT1-MMP regulates synovial

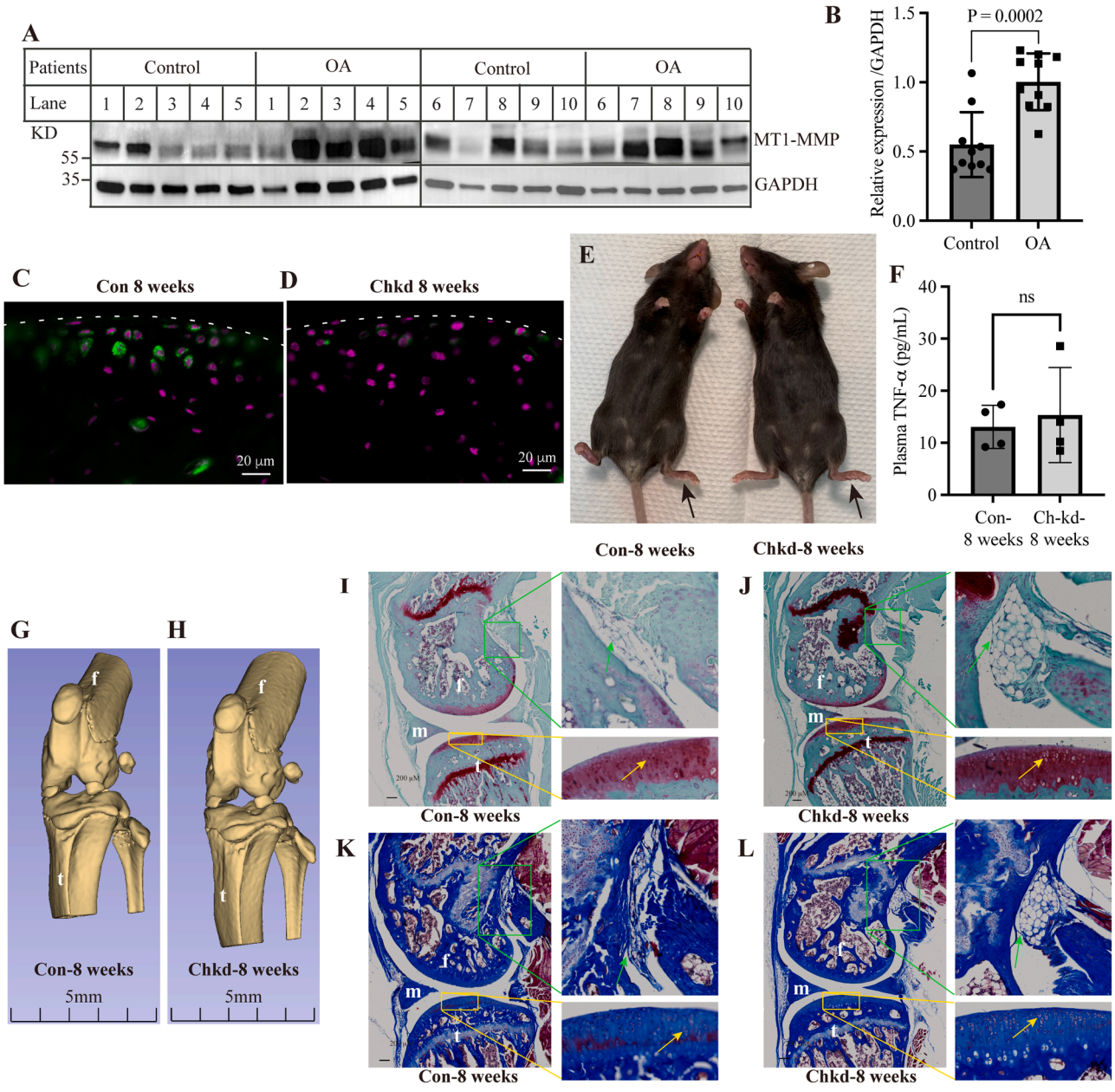

Fig. 3. MT1-MMP Expression and *Mmp14*^{chkd} mice. A and B. Immunoblotting of MT1-MMP in human patient samples. Relative densitometry was defined as the ratio of the densitometry of MT1-MMP to that of GAPDH in the same sample. **C and D.** Immunofluorescence of the joint surface. Mice (10–12 weeks old) were injected with olive oil (Con) or tamoxifen (Chkd) and then analyzed at the indicated time of post-injection. Green fluorescence indicates MT1-MMP, contrasted with violet-DAPI stained nuclei ($n = 3$). **E.** Picture of mice 8 weeks post-injection. **F.** Plasma TNF-α levels (con, $n = 4$; KD, $n = 4$). **G and H**. Reconstruction of μCT images ($n = 4$). **I-L.** Images of Safranin O/Fast Green (Fisher Scientific, S-670) and Masson's trichrome (StatLab, KTMTRPT) staining with enlarged views showing synovial membrane (green arrows) and chondrocytes (yellow arrows) ($n = 5$). Representative images were shown. Similar results were observed in other samples in the same group. ns=no significant. f, femur; m, meniscus; t, tibia.

fibrosis and its contribution to the development of arthritis.

Constitutive *Mmp14* knockout mice showed severe growth impairment and started to die shortly after birth, primarily due to wasting [8, 9]. Conversely, *Mmp14*^{kd} mice were not significantly different from control mice except for a form of severe inflammatory arthritis, which was the sole reason for reaching a humane endpoint. *Mmp14*^{kd} mice also gained comparable body weight, displayed similar blood glucose, and plasma triglyceride (TG) levels as control mice 6 weeks after tamoxifen administration (**Figures S3A to C**). Plasma total cholesterol (TC) levels trended downward in *Mmp14*^{kd} mice (**Figure S3D)**, but did not reach statistical significance, which differed from our previous findings in *Mmp14* liver-specific knockout mice that showed a slight but significant reduction in plasma TC levels [3]. *Mmp14*^{kd} mice had significantly elevated plasma TNF-α levels, which might have contributed to the discrepancy between the two studies because TNF-α affects lipid metabolism [18]. Nevertheless, global MT1-MMP deficiency in adult mice does not significantly change baseline metabolic characteristics but leads to a form of severe inflammatory arthritis, suggesting that highly cell-type specific rather than systemic pharmacological inhibition of MT1-MMP would be required to make it safe for potential clinical use.

Chondrocyte-specific Mmp14 conditional knockout mice

Articular chondrocytes express MT1-MMP, which degrades aggrecan and collagen directly, or indirectly through activation of MMP13 [19, 20]. Studies in constitutive *Mmp14* knockout mice showed that lacking MT1-MMP significantly reduced chondrocyte proliferation [9]. We, on the other hand, observed apparent chondrocyte hypertrophy when MT1-MMP was deficient in *Mmp14*^{kd} adult mice. To understand the role of chondrocyte *Mmp14* in the development of arthritis, we first examined MT1-MMP expression in human cartilage samples. Ten articular cartilage samples were collected from OA patients undergoing joint replacement. The mean relative expression of MT1-MMP in the OA group was 1.003 ± 0.21 (Figs. 3**A and B**). We also collected ten cartilage samples from patients without OA as the control. The relative expression of MT1-MMP in the control group was 0.55 ± 0.23 ($p = 0.0002$ *vs* the OA group). Of note, due to limitations in sample availability, the control group included cartilages from fingers, knees, elbows, and hips, with only two knee samples. Furthermore, most samples in the OA group were from older females, whereas the control group included male and female patients with a wide age range (**Table S1**). The expression of MT1-MMP is regulated differentially by sex, age, and location, which may contribute to the observed difference between the OA and the control group. Nevertheless, we detected substantial expression of MT1-MMP in articular cartilage samples in the OA group, which could either damage ECM and accelerate disease progression, or restore ECM homeostasis as a compensatory mechanism. To address these possibilities, we developed chondrocyte-specific *Mmp14* tamoxifen-induced conditional knockout mice using *Mmp14*^{flox} mice and procollagen type II, alpha1 (Col2a1)-CreER^{T} mice, as described in previous studies [21, 22].

The expression of Cre-ER^{T} is driven by endogenous *Col2a1* promoter that is highly expressed in chondrocytes (**Figure S4A**). Homozygous *Col2a1*-Cre/ER^{T}-*Mmp14*^{flox} mice contained floxed *Mmp14* and Cre-ER^{T}, whereas heterozygous mice had the Cre and both wild-type and floxed *Mmp14* bands (**Figure S4B**). Adult homozygous mice were administered tamoxifen to generate chondrocyte-specific *Mmp14*-deficient mice (*Mmp14*^{chkd}), or olive oil in control mice. A 693 bp PCR product of Cre-mediated recombination of the *Mmp14* gene was only detected in the articular cartilage of *Mmp14*^{chkd} mice, but not in the cartilage of control mice or in other tissues of control and *Mmp14*^{chkd} mice, indicating specific conditional knockout of *Mmp14* in chondrocytes (**Figure S4C**). MT1-MMP signal was also markedly reduced in cartilage cells of *Mmp14*^{chkd} and *Mmp14*^{kd} mice (Figs. 3**C and D, and S5A**), indicating efficient chondrocyte *Mmp14* reduction.

Unlike *Mmp14*^{kd} mice, *Mmp14*^{chkd} mice did not develop noticeable arthritis (Fig. 3**E**), and their plasma TNF-α levels were comparable to those of control mice (Fig. 3**F**). μCT also showed no apparent subchondral bone remodeling in *Mmp14*^{chkd} mice (Figs. 3**G and H**). Body weight and blood glucose levels were also comparable in the two groups (**Figures S5B and C**). Detailed analysis of mouse joints revealed noticeable chondrocyte hypertrophy (**yellow arrows**) but no synovial hyperplasia or fibrosis (**green arrows**) in *Mmp14*^{chkd} mice (Figs. 3**I-L**). To further confirm these findings, we sectioned joint samples to assess the synovial membrane around the infrapatellar fat pad (**Figures S6A and B**). Consistent with results shown in Fig. 2, most adipocytes in the infrapatellar fat pad of *Mmp14*^{kd} mice virtually disappeared and were replaced by collagen fibers, indicating fibrosis. In contrast, both control and *Mmp14*^{chkd} mice showed a clear infrapatellar fat pad and normal synovial lining. We also assessed the levels of MMP13 and COLX, which are known makers of hypertrophic chondrocytes. As shown in **Figure S7A**, *Mmp14* deficiency increased MMP13 expression in chondrocytes of *Mmp14*^{kd} and *Mmp14*^{chkd} mice. On the other hand, COLX displayed a diffuse increase in chondrocytes from *Mmp14*^{kd} mice but not from *Mmp14*^{chkd} mice (**Figure S7B**), suggesting that *Mmp14*^{kd} mice had greater chondrocyte hypertrophy compared with *Mmp14*^{chkd} mice. Nevertheless, lack of chondrocyte MT1-MMP does not cause overt arthritis, suggesting that lack of MT1-MMP in cell types other than chondrocytes MT1-MMP, or in multiple cell types, is the main driver in the initiation of inflammatory arthritis observed in adult *Mmp14*^{kd} mice. However, we cannot exclude that chondrocyte MT1-MMP deficiency contributes to disease progression later, as the severely damaged joints in adult *Mmp14*^{kd} mice had concomitant deficiency of MT1-MMP in chondrocytes and other cell types.

It is worth noting that conditional knockout efficiency of target genes in the Cre-Lox system is affected by the level of Cre recombinase. The expression of Cre in the global and chondrocyte-specific *Mmp14* deficient mice was controlled by the endogenous mouse ROSA26 and Col2a1 promoter, respectively, which might lead to differences in Cre expression and *Mmp14* conditional knockout in the two strains. In addition to the Cre recombinase levels, the type of Cre-recombinase differed between the two mouse models, where *Mmp14*^{kd} utilized the Cre-ER^{T2}, and the *Mmp14*^{chkd}, Cre-ER^{T}, which are known to have differences in terms of their sensitivity to induced activation [23]. Although expression of MT1-MMP was substantially reduced in chondrocytes of both *Mmp14*^{kd} and *Mmp14*^{chkd} mice compared with control mice, we cannot rule out the possibility that the remaining level of chondrocyte MT1-MMP in *Mmp14*^{chkd} mice was higher than that in *Mmp14*^{kd} mice, which might contribute to the observed difference between the two strains.

Determining the mechanism underlying the causes of severe arthritis in *Mmp14*^{kd} mice is challenging because MT1-MMP is ubiquitously expressed and its deficiency affects multiple tissues and cell types. LDLR-related protein 1 (LRP1) in chondrocytes has been reported to play an important role in OA development. Knockdown of LRP1 in cultured human chondrocytes led to cell death [24]. Furthermore, chondrocyte LRP1 mediated endocytosis of ADAMTs-4 and 5, and MMP-13 to reduce cartilage degradation. LRP1 shedding was increased in OA, leading to reduced endocytosis of these metalloproteinases and subsequently enhanced cartilage degradation. Chondrocyte LRP1 was mainly shed by ADAM17 and MT1-MMP. Inhibition of MT1-MMP or ADAM17 alone partially suppressed LRP1 shedding, while combined inhibition of MT1-MMP and ADAM17 markedly blocked LRP1 shedding and inhibited cartilage matrix degradation [25]. Therefore, chondrocyte MT1-MMP deficiency might partially inhibit LRP1 shedding, thereby modulating OA development and progression. To test this possibility, we examined LRP1 and found that its levels were not obviously changed in chondrocytes of *Mmp14*^{kd} and *Mmp14*^{Chkd} mice (**Figure S7C**), suggesting that the LRP1 pathway may not be a significant contributor to the effect of *Mmp14* deficiency on arthritis and chondrocytes.

How MT1-MMP deficiency causes synovial fibrosis and chondrocyte hypertrophy is unclear. MT1-MMP plays a key role in maintaining tissue

ECM homeostasis. Disruption of ECM homeostasis, such as changes in ECM components and their interactions, alters ECM structure and biophysical properties and leads to various pathological conditions. For example, ECM-derived damage-associated molecular patterns activate toll-like receptors (TLRs) and inflammasome formation [26]. In addition, TGF-β plays an important role in the development of fibrosis and hypertrophy [27,28], and the level of its active form is high in synovial fluid of patients with RA and OA [29]. Latent TGF-β activation is affected by changes in ECMs, such as rigidity and components, which may be directly or indirectly affected by MT1-MMP deficiency. The FGF-2 signaling pathway also plays a role in chondrocyte hypertrophy [28]. Knockout of MT1-MMP reduced FGF-2 signaling in osteoblasts [30], suggesting a regulatory role of MT1-MMP in the FGF-2 pathway in chondrocytes. Experiments are ongoing to investigate these possibilities.

Mice with global conditional knockout of MT1-MMP showed joint swelling, synovial inflammation, fibrosis, and hypertrophic chondrocytes. Rheumatoid arthritis (RA) is an autoimmune disease. In RA, the immune system attacks the synovium, causing synovitis, swollen joints, activation of fibroblast-like synoviocytes and synovial fibrosis. Hyperproliferation of fibroblast-like synoviocytes perpetuates joint, cartilage and bone damage. On the other hand, osteoarthritis is primarily caused by cartilage proteolytic destruction. One of the key indicators of OA is chondrocyte hypertrophy. However, advanced OA also displays synovial inflammation, fibrosis and bone remodeling [27]. In addition, both RA and OA are chronic progressive diseases. *Mmp14*^{kd} mice rapidly developed severe arthritis. Therefore, the development of severe arthritis in *Mmp14*^{kd} mice is probably multifactorial, associated with features of both OA and RA.

Miller et al. reported that MT1-MMP mediated synovial fibroblast invasion and promoted pannus invasion in human RA, suggesting the potential of MT1-MMP inhibition as a treatment for RA [7]. With respect to the articular cartilage, we observed substantial expression of MT1-MMP in human OA cartilages. Given that COLII is the main component of cartilage and MT1-MMP can proteolytically cleave COLII [31], we evaluated cartilage COLII (**Figure S7D**). *Mmp14*^{chkd} but not *Mmp14*^{kd} mice, displayed an apparent increase in COLII in the deep zone. MT1-MMP was specifically reduced in *Col-2* expressing cells in *Mmp14*^{chkd} mice, which might reduce COLII degradation. MT1-MMP was also deficient in chondrocytes of *Mmp14*^{kd} mice. However, load-bearing from movement is necessary for appropriate cartilage remodeling that involves COLII production and degradation [32]. The joint stiffness in *Mmp14*^{kd} mice impaired their movement, and likely the biomechanical property of cartilage, which could affect cartilage remodeling and COLII production. Nevertheless, our findings indicate that global MT1-MMP deficiency in adult mice leads to synovial fibrosis and arthritis. Chondrocyte-specific MT1-MMP deficiency in adult mice resulted in chondrocyte hypertrophy, even with increased cartilage COLII content and no overt arthritis. Taken together, these findings indicate that a delicate balance of MT1-MMP activity in different joint compartments is required to maintain healthy joint function. Therefore, a major challenge for the use of MT1-MMP inhibition in treating arthritis is how to precisely control MT1-MMP activity to an optimal level for the benefit of patients with arthritis. More research is urgently in need to understand the underlying mechanisms of MT1-MMP in the pathogenesis of arthritis.

Experimental procedures

Animal

Mmp14^{flox} mice were generated as described [3] and then crossed with mice expressing tamoxifen-inducible Cre-ER^{T2} or Cre-ER^{T}, under the control of the endogenous mouse Gt(ROSA)26Sor or Col2a1 to generate inducible global or chondrocyte *Mmp14* deficient mice, respectively. Genotyping primers were in **Table S2.** Mice were housed at the University of Alberta and fed a standard chow diet ad libitum. Cre recombinase activation was induced by intraperitoneal injection of tamoxifen (75 mg/kg/day dissolved in olive oil for 5 consecutive days). Control mice were injected with olive oil for the same time period. All animal procedures were approved by the University of Alberta's Animal Care and Use Committee and were conducted in accordance with the guidelines of the Canadian Council on Animal Care.

qRT-PCR and blood parameters

Total RNAs were extracted from mouse tissues using TRIzol® and then treated with RNase-free DNase I (NEB). Two micrograms of RNA were used for synthesizing cDNA using the High Capacity cDNA Reverse Transcription Kit. qRT-PCR was carried out using SYBR®Select Master Mix. Relative gene expression was normalized to *Gapdh*. Primers are listed in **Table S2**. Fasting plasma TG, TC and TNF-α levels were measured using specific colorimetric kits. Fasting blood glucose was measured using a blood glucometer.

Joint flexibility and arthritis scores

The angle of the fully extended joint of each mouse was measured. Control mice had an average angle of 145°. The loss of flexibility was calculated by subtracting the angle of a fully extended joint of each *Mmp14*^{kd} mouse from 145, which was then divided by 145 to calculate the percentage of flexibility loss. Arthritis scores were calculated as described [15]. Total score of each mouse was the sum of its 4 paws.

Histochemistry and immunoblotting

Samples were fixed, decalcified, embedded in paraffin, and sectioned at 7 μm thickness. Slides were deparaffinized, and rehydrated as described [33]. Sections were then stained with Safranin O/Fast Green or Masson's trichrome solution and imaged on a microscope. Slides were also incubated with a primary antibody as indicated after antigen retrieval, as described [34], followed by an Alexa Fluor 647 donkey anti-rabbit IgG and a fluorescence microscope. Homogenate of cartilage samples was subjected to immunoblotting with an anti-MT1-MMP antibody. Relative densitometry was determined and normalized on a ChemiDoc™ Gel Image System. Antibody information was included in **Table S3**.

μCT analysis

Mice anesthetized were scanned on a MILabs μCT using the following setting: voxel size = 10 μm; voltage = 50 kV; current = 0.24 mA; and exposure time = 75 ms, as described [34]. Scans were reconstructed at a voxel size of 25 μm, analyzed, and modeled using the AVIZO 3D software.

Human patient samples

All experimental methods conform to the principles of the Declaration of Helsinki. The collection and processing of human tissue samples were approved by the medical ethics committee at the Sixth Affiliated Hospital of Guangzhou Medical University (Qingyuan People's Hospital; IRB-2022–081). Patients were fully informed, and specimens were collected after written informed consent.

10 cartilage samples were collected from OA patients with knee osteoarthritis undergoing joint replacement. Patients with purulent arthritis, gouty arthritis, RA, chorionic pigmented arthritis, or other autoimmune disease were excluded. 10 control cartilage samples were collected from patients with hip fractures, congenital malformation, or traumatic amputation (**Table S1**).

Statistical analysis

Prism 9 was used for all statistical analyses. Student's *t*-test was used to determine significant differences between two groups. Each group contained at least three biological replicates unless otherwise stated. Both male and female mice were used in each group, and no significant difference was observed between male and female mice. All data were presented as mean ± S.D. The significance was defined as * $p<0.05$.

Author contributions

DWZ designed the experiments, analyzed data, supervised and directed this project, and wrote the manuscript. XDX, GG, HL and DR performed experiments, collected and analyzed data, provided discussions and comments, and participated in manuscript writing. HMG, XJW, FYS, AA, MA, and ZZ performed experiments and provided technical support. GQW and DG supervised this project, provided technical support, guidance, discussions, and comments, and participated in manuscript writing.

Declaration of Competing Interest

The authors have declared no conflict of interest.

Data availability

Data will be made available on request.

Acknowledgement

This work was supported by the Canadian Institutes of Health Research (PS 155994) and the Natural Science Foundation of Guangdong Province (2022A1515012449). The authors thanked the Lipidomics Core (RRID:SCR_019176) and the Transgenic Core (RRID: SCR_019175) of the Faculty of Medicine and Dentistry at the University of Alberta. GG was partly supported by the MatCH program that is funded by the generosity of the Stollery Children's Hospital Foundation and supporters of the Alberta Women's Health Foundation through the Women and Children's Health Research Institute.

Supplementary materials

Supplementary material associated with this article can be found, in the online version, at doi:10.1016/j.matbio.2023.08.003.

References

[1] V. Gifford, Y. Itoh, MT1-MMP-dependent cell migration: proteolytic and non-proteolytic mechanisms, Biochem. Soc. Trans. 47 (3) (2019) 811–826.
[2] X.D. Xia, A. Alabi, M. Wang, H.M. Gu, R.Z. Yang, G. Wang, D.W. Zhang, Membrane-type I matrix metalloproteinase (MT1-MMP), lipid metabolism and therapeutic implications, J. Mol. Cell Biol. 13 (7) (2021) 513–526.
[3] A. Alabi, X.D. Xia, H.M. Gu, F. Wang, S.J. Deng, N. Yang, A. Adijiang, D.N. Douglas, N.M. Kneteman, Y. Xue, L. Chen, S. Qin, G. Wang, D.W. Zhang, Membrane type 1 matrix metalloproteinase promotes LDL receptor shedding and accelerates the development of atherosclerosis, Nat. Commun. 12 (1) (2021) 1889.
[4] X. Guo, P. Asthana, S. Gurung, S. Zhang, S.K.K. Wong, S. Fallah, C.F.W. Chow, S. Che, L. Zhai, Z. Wang, X. Ge, Z. Jiang, J. Wu, Y. Zhang, X. Wu, K. Xu, C.Y. Lin, H. Y. Kwan, A. Lyu, Z. Zhou, Z.X. Bian, H.L.X. Wong, Regulation of age-associated insulin resistance by MT1-MMP-mediated cleavage of insulin receptor, Nat. Commun. 13 (1) (2022) 3749.
[5] C.F.W. Chow, X. Guo, P. Asthana, S. Zhang, S.K.K. Wong, S. Fallah, S. Che, S. Gurung, Z. Wang, K.B. Lee, X. Ge, S. Yuan, H. Xu, J.P.K. Ip, Z. Jiang, L. Zhai, J. Wu, Y. Zhang, A.K. Mahato, M. Saarma, C.Y. Lin, H.Y. Kwan, T. Huang, A. Lyu, Z. Zhou, Z.X. Bian, H.L.X. Wong, Body weight regulation via MT1-MMP-mediated cleavage of GFRAL, Nat Metab 4 (2) (2022) 203–212.
[6] H. Yamanaka, K. Makino, M. Takizawa, H. Nakamura, N. Fujimoto, H. Moriya, R. Nemori, H. Sato, M. Seiki, Y. Okada, Expression and tissue localization of membrane-types 1, 2, and 3 matrix metalloproteinases in rheumatoid synovium, Lab. Invest. 80 (5) (2000) 677–687.
[7] M.C. Miller, H.B. Manning, A. Jain, L. Troeberg, J. Dudhia, D. Essex, A. Sandison, M. Seiki, J. Nanchahal, H. Nagase, Y. Itoh, Membrane type 1 matrix metalloproteinase is a crucial promoter of synovial invasion in human rheumatoid arthritis, Arthritis Rheum. 60 (3) (2009) 686–697.
[8] Z. Zhou, S.S. Apte, R. Soininen, R. Cao, G.Y. Baaklini, R.W. Rauser, J. Wang, Y. Cao, K. Tryggvason, Impaired endochondral ossification and angiogenesis in mice deficient in membrane-type matrix metalloproteinase I, Proc. Natl. Acad. Sci. USA. 97 (8) (2000) 4052–4057.
[9] K. Holmbeck, P. Bianco, J. Caterina, S. Yamada, M. Kromer, S.A. Kuznetsov, M. Mankani, P.G. Robey, A.R. Poole, I. Pidoux, J.M. Ward, H. Birkedal-Hansen, MT1-MMP-deficient mice develop dwarfism, osteopenia, arthritis, and connective tissue disease due to inadequate collagen turnover, Cell 99 (1) (1999) 81–92.
[10] D.P. Becker, T.E. Barta, L.J. Bedell, T.L. Boehm, B.R. Bond, J. Carroll, C.P. Carron, G.A. Decrescenzo, A.M. Easton, J.N. Freskos, C.L. Funckes-Shippy, M. Heron, S. Hockerman, C.P. Howard, J.R. Kiefer, M.H. Li, K.J. Mathis, J.J. McDonald, P. P. Mehta, G.E. Munie, T. Sunyer, C.A. Swearingen, C.I. Villamil, D. Welsch, J. M. Williams, Y. Yu, J. Yao, Orally active MMP-1 sparing alpha-tetrahydropyranyl and alpha-piperidinyl sulfone matrix metalloproteinase (MMP) inhibitors with efficacy in cancer, arthritis, and cardiovascular disease, J. Med. Chem. 53 (18) (2010) 6653–6680.
[11] G.B. Fields, The Rebirth of Matrix Metalloproteinase Inhibitors: moving Beyond the Dogma, Cells 8 (9) (2019).
[12] T. Fischer, R. Riedl, Inhibitory Antibodies Designed for Matrix Metalloproteinase Modulation, Molecules 24 (12) (2019).
[13] A. Klose, P. Zigrino, C. Mauch, Monocyte/macrophage MMP-14 modulates cell infiltration and T-cell attraction in contact dermatitis but not in murine wound healing, Am. J. Pathol. 182 (3) (2013) 755–764.
[14] P. Zigrino, O. Ayachi, A. Schild, J. Kaltenberg, J. Zamek, R. Nischt, M. Koch, C. Mauch, Loss of epidermal MMP-14 expression interferes with angiogenesis but not with re-epithelialization, Eur. J. Cell Biol. 91 (10) (2012) 748–756.
[15] P. Hawkins, R. Armstrong, T. Boden, P. Garside, K. Knight, E. Lilley, M. Seed, M. Wilkinson, R.O. Williams, Applying refinement to the use of mice and rats in rheumatoid arthritis research, Inflammopharmacology 23 (4) (2015) 131–150.
[16] L.K. Bai, Y.Z. Su, X.X. Wang, B. Bai, C.Q. Zhang, L.Y. Zhang, G.L. Zhang, Synovial Macrophages: past Life, Current Situation, and Application in Inflammatory Arthritis, Front. Immunol. 13 (2022), 905356.
[17] L.C. Huber, O. Distler, I. Tarner, R.E. Gay, S. Gay, T. Pap, Synovial fibroblasts: key players in rheumatoid arthritis, Rheumatology (Oxford) 45 (6) (2006) 669–675.
[18] J.K. Sethi, G.S. Hotamisligil, Metabolic Messengers: tumour necrosis factor, Nat Metab 3 (10) (2021) 1302–1312.
[19] S. Chubinskaya, K.E. Kuettner, A.A. Cole, Expression of matrix metalloproteinases in normal and damaged articular cartilage from human knee and ankle joints, Lab. Invest. 79 (12) (1999) 1669–1677.
[20] Y. Itoh, Membrane-type matrix metalloproteinases: their functions and regulations, Matrix Biol. 44-46 (2015) 207–223.
[21] M. Zhu, M. Chen, A.C. Lichtler, R.J. O'Keefe, D. Chen, Tamoxifen-inducible Cre-recombination in articular chondrocytes of adult Col2a1-CreER(T2) transgenic mice, Osteoarthritis Cartilage 16 (1) (2008) 129–130.
[22] M. Chen, A.C. Lichtler, T.J. Sheu, C. Xie, X. Zhang, R.J. O'Keefe, D. Chen, Generation of a transgenic mouse model with chondrocyte-specific and tamoxifen-inducible expression of Cre recombinase, Genesis 45 (1) (2007) 44–50.
[23] A.K. Indra, X. Warot, J. Brocard, J.M. Bornert, J.H. Xiao, P. Chambon, D. Metzger, Temporally-controlled site-specific mutagenesis in the basal layer of the epidermis: comparison of the recombinase activity of the tamoxifen-inducible Cre-ER(T) and Cre-ER(T2) recombinases, Nucleic. Acids. Res. 27 (22) (1999) 4324–4327.
[24] K. Yamamoto, C. Scavenius, M.M. Meschis, A.M.E. Gremida, E.H. Mogensen, I. B. Thogersen, S. Bonelli, S.D. Scilabra, A. Jensen, S. Santamaria, J. Ahnstrom, G. Bou-Gharios, J.J. Enghild, H. Nagase, A top-down approach to uncover the hidden ligandome of low-density lipoprotein receptor-related protein 1 in cartilage, Matrix Biol. 112 (2022) 190–218.
[25] K. Yamamoto, S. Santamaria, K.A. Botkjaer, J. Dudhia, L. Troeberg, Y. Itoh, G. Murphy, H. Nagase, Inhibition of Shedding of Low-Density Lipoprotein Receptor-Related Protein 1 Reverses Cartilage Matrix Degradation in Osteoarthritis, Arthritis Rheumatol 69 (6) (2017) 1246–1256.
[26] E. Ramos-Tovar, P. Muriel, Molecular mechanisms that link oxidative stress, inflammation, and fibrosis in the liver, Antioxidants 9 (12) (2020), 1279-1279.
[27] L. Zhang, R. Xing, Z. Huang, L. Ding, L. Zhang, M. Li, X. Li, P. Wang, J. Mao, Synovial fibrosis involvement in osteoarthritis, Front Med 8 (2021), 684389.
[28] Q. Yao, X. Wu, C. Tao, W. Gong, M. Chen, M. Qu, Y. Zhong, T. He, S. Chen, G. Xiao, Osteoarthritis: pathogenic signaling pathways and therapeutic targets, Signal Transduct Target Ther 8 (1) (2023) 56.
[29] R. Fava, N. Olsen, J. Keski-Oja, H. Moses, T. Pincus, Active and latent forms of transforming growth factor beta activity in synovial effusions, J. Exp. Med. 169 (1) (1989) 291–296.
[30] K.M. Chan, H.L. Wong, G. Jin, B. Liu, R. Cao, Y. Cao, K. Lehti, K. Tryggvason, Z. Zhou, MT1-MMP inactivates ADAM9 to regulate FGFR2 signaling and calvarial osteogenesis, Dev. Cell 22 (6) (2012) 1176–1190.
[31] E. Ohuchi, K. Imai, Y. Fujii, H. Sato, M. Seiki, Y. Okada, Membrane type 1 matrix metalloproteinase digests interstitial collagens and other extracellular matrix macromolecules, J. Biol. Chem. 272 (4) (1997) 2446–2451.

[32] Z. Peng, H. Sun, V. Bunpetch, Y. Koh, Y. Wen, D. Wu, H. Ouyang, The regulation of cartilage extracellular matrix homeostasis in joint cartilage degeneration and regeneration, Biomaterials 268 (2021), 120555.
[33] D.M. Roth, L. Puttagunta, D. Graf, Histological Techniques for Sectioning Bones of the Vertebrate Craniofacial Skeleton, Methods Mol. Biol. 2403 (2022) 187–200.
[34] Z. Malik, D.M. Roth, F. Eaton, J.M. Theodor, D. Graf, Mesenchymal Bmp7 Controls Onset of Tooth Mineralization: a Novel Way to Regulate Molar Cusp Shape, Front Physiol 11 (2020) 698.